Commun. Theor. Phys. **70** (2018) 303–310 Vol. 70, No. 3, September 1, 2018

Universal Pseudo-$\mathcal{PT}$-Antisymmetry on One-Dimensional Atomic Optical Lattices*

Xin Wang (王欣)[1,†] and Chang-Pu Sun (孙昌璞)[1,2]

[1]Beijing Computational Science Research Center, Beijing 100193, China

[2]Graduate School, China Academy of Engineering Physics, Beijing 100193, China

(Received February 11, 2018; revised manuscript received May 22, 2018)

Abstract *We present the interesting result that under sinusoidal field detuning setting along the propagation direction of 1D atomic lattices, the probe susceptibility response of the lattices, regardless of atomic configuration, uniformly demonstrates pseudo-$\mathcal{PT}$-antisymmetry, which by our definition corresponds to $n(z) = -n^*(-z)$, the complex refractive index antisymmetry along propagation axis, and when being cast back to quantum mechanical side, corresponds to $V(x,t) = -V^*(x,-t)$, the conjugate time-reversal antisymmetry of complex potential. We define this as the pseudo-$\mathcal{PT}$-antisymmetry, and prove the reason for this phenomenon to be the quantum-mechanical nature described by master equation under weak field approximation for any configuration of 1D atomic lattices. This work will help to deepen the understanding of origin of optical response features of atomic lattices, and will certainly open up the gate to a more rigorous, durable and flexible method of atomic optical lattice design.*

DOI: 10.1088/0253-6102/70/3/303

Key words: pseudo-$\mathcal{PT}$-antisymmetry, conjugate time-reversal antisymmetry, zigzag-type atom configuration

1 Introduction

Since the concept of $\mathcal{PT}$-symmetry was raised by Bender and co-workers,[1−2] in the past decade there has been growing interest in the study of this area due to the fact that non-Hermitian $\mathcal{PT}$-symmetric Hamiltonian extends the framework of quantum mechanics into the complex domain. Although in recent years much work has been done on the theoretical side of this issue,[3−12] up till this day, there has not been genuine experimental realization of $\mathcal{PT}$-symmetric quantum system yet, because the $\mathcal{PT}$-symmetry requires $V(x) = V^*(-x)$ for one-dimensional Hamiltonian, which demands existence of complex potential for the system, something hard to realize despite the theoretical proposal.

Fortunately, the study of $\mathcal{PT}$-symmetry found its cast in the field of optics, thanks to the isomorphism between Schrödinger equation and optical paraxial wave equation. For this reason, many endeavors have shown up in realizing $\mathcal{PT}$-symmetric optical metamaterials in recent years. On one hand, artificial optical materials have already shown the advantages for achieving unusual electromagnetic properties compared to natural media, not to mention the fact that the $\mathcal{PT}$-symmetry will certainly open up the gate to more intriguing properties, like double refraction and band merging,[13−14] power oscillations,[15−16] coherent perfect absorbers,[17−19] unidirectional invisibility,[14,20−21] and so on. However as a matter of fact, most of these works are carried out on solid-state optical systems, without much attempt to utilize atomic lattices. Considering that atomic optical lattices have their big advantages in real-time, all-optical tunable and reconfigurable features in control as compared to solid-state systems, it is of valuable importance to extend the study of $\mathcal{PT}$-symmetry to this area. In recent years several works have come into sight[22−26] on this aspect.

For study of $\mathcal{PT}$-symmetry in optical field, when mapping the time-dependent Schrödinger equation to the paraxial wave propagation equation, the role of time variable t in Schrödinger equation is cast to the spatial variable of propagation direction (we use z in this work) in paraxial wave equation, and the $\mathcal{PT}$-symmetry condition $V(x) = V^*(-x)$ is mapped to the complex refractive index symmetry $n(x) = n^*(-x)$ in transverse plane of propagation. Many works have been done under this scheme.[15−16,27−33]

On the other hand, the question has been asked about what if we implant the symmetric modulation of complex refractive index n to the longitudinal direction instead of transverse plane of optical wave propagation.[34] Inspired by this, we propose the scheme of realizing complex refractive index symmetry along the propagation direction of one-dimensional atomic optical lattices.

Surprisingly and most interestingly, in our study we find that under spatial sinusoidal detuning setting along propagation direction, 1D atomic lattices of any configuration could uniformly demonstrate pseudo-$\mathcal{PT}$-antisymmetry, by which we mean $n(z) = -n^*(-z)$, where

*Support from National Basic Research Program of China under Grant No. 2014CB921403, National Natural Science Foundation of China under Grant Nos. 11534002, U1730449 and U1530401

†Corresponding author, E-mail: xwang@csrc.ac.cn

z denotes the propagation axis. When being cast back to quantum-mechanical side, this corresponds to $V(x,t) = -V^*(x,-t)$, the conjugate time-reversal antisymmetry of complex potential $V(x,t)$ in Schrödinger equation.

The phenomenon of universal inducement of pseudo-$\mathcal{PT}$-antisymmetry goes beyond our usual recognition that the optical features of atomic lattices are predominantly related to the energy level configuration of atoms, which together with particular setting of applied fields determine the optical response features of the lattice. Rather, it must originate from some fundamental physical features in the atomic optical lattice system, so that it could not see the difference between configuration details. And we find that the reason for this phenomenon is the quantum-mechanical nature described by master equation under weak probe field approximation.

The article is organized as follows. In Sec. 2 we define the concept of pseudo-$\mathcal{PT}$-antisymmetry. In Sec. 3 we give the proof of universal inducement of pseudo-$\mathcal{PT}$-antisymmetry under spatial sinusoidal detuning setting. In Sec. 4 we present an example of pseudo-$\mathcal{PT}$-antisymmetry inducement on the family of zigzag-type configurations. And finally in Sec. 5 we conclude the article.

2 Pseudo-$\mathcal{PT}$-antisymmetry

The effects of parity operator $\hat{\mathcal{P}}$ and time-reversal operator $\hat{\mathcal{T}}$ on quantum-mechanical coordinate operator $\hat{x}$ and momentum operator $\hat{p}$ are

$$\begin{aligned} &\hat{\mathcal{P}} : \hat{p} \to -\hat{p}, \hat{x} \to -\hat{x}\,, \\ &\hat{\mathcal{T}} : \hat{p} \to -\hat{p}, \hat{x} \to \hat{x}, i \to -i\,, \end{aligned} \tag{1}$$

with $\hat{\mathcal{P}}^2 = \hat{\mathcal{T}}^2 = 1$ and $\hat{\mathcal{P}}$, $\hat{\mathcal{T}}$ commute with each other. Since a $\mathcal{PT}$-reflected Hamiltonian is defined as $\hat{H}^{\hat{\mathcal{P}}\hat{\mathcal{T}}} = \hat{\mathcal{P}}\hat{\mathcal{T}}\hat{H}\hat{\mathcal{P}}\hat{\mathcal{T}}$ and the $\mathcal{PT}$-symmetry requires that $\hat{H} = \hat{H}^{\hat{\mathcal{P}}\hat{\mathcal{T}}}$, for one-dimensional Hamiltonian $\hat{H} = \hat{p}^2/2m + V(\hat{x})$, the $\mathcal{PT}$-symmetry comes down to

$$V(x) = V^*(-x)\,. \tag{2}$$

This suggests a complex potential setting, which is not normally applicable in physical experimental environment. However the complex potential V has found its cast in the complex refractive index n in optics.

Optical lattice can be looked on as non-magnetic medium with no free charges or currents in it, then for electric field propagation we have the Helmholtz equation

$$\Big[\nabla^2 + \frac{\omega^2}{c^2} n^2\Big] \boldsymbol{E}(\vec{x}, z) = 0\,, \tag{3}$$

where z is the variable on propagation axis of 1D atomic lattices, $\vec{x}$ stands for any vector in transverse plane, ω the angular frequency of the electromagnetic wave oscillation, and c the speed of light in vacuum. In homogeneous media, Eq. (3) reduces to a scalar equation.

In our one-dimensional optical lattice model, n could be designed as the periodic function of z, i.e. $n(z+a) = n(z)$, where a is the spatial period of 1D optical lattice. Including the real background refractive index n_0, we have $n(z) = n_0 + \delta n(z)$, with $\delta n(z) = n_R(z) + i n_I(z)$ being complex and $|\delta n(z)| \ll |n_0|$. The propagating electric field is given by $E(x,z) = \phi(x,z)\,\mathrm{e}^{\mathrm{i}k_0 z}$, where $\phi(x,z)$ is the envelope function. Then under paraxial approximation, the scalar Helmholtz equation reduces to

$$[\partial_x^2 + 2\mathrm{i}k_0\partial_z + V(z)]\phi(x,z) = 0\,, \tag{4}$$

where $k_0 = n_0\omega/c$, $V(z) = 2(k_0^2/n_0)\delta n(z)$ is the effective potential. Notice however, that Eq. (4) is not the analog of one-dimensional Schrödinger equation

$$\Big[-\frac{\hbar^2}{2m}\partial_x^2 - \mathrm{i}\hbar\partial_t + V(x)\Big]\psi(x,t) = 0\,, \tag{5}$$

because the genuine analog requires that time variable t in Eq. (5) be cast to longitudinal variable z in paraxial wave equation, and spatial variable x in Eq. (5) be cast to transverse variable x, which is to say, V in Eq. (4) should be a function of x, not a function of z. This means the normal $\mathcal{PT}$-symmetry requires the complex refractive index to satisfy $\delta n(x) = \delta n^*(-x)$ in transverse plane, with no restriction set for z direction for 1D optical lattices. Compared to this, what we realized in this paper is $\delta n(z) = -\delta n^*(-z)$ along the propagation direction of 1D atomic lattices. From the point of view of $\mathcal{PT}$-symmetry, $\delta n(z) = -\delta n^*(-z)$ corresponds to the condition

$$V(x,t) = -V^*(x,-t)\,, \tag{6}$$

which is the conjugate time-reversal antisymmetry of complex potential $V(x,t)$, and we call it pseudo-$\mathcal{PT}$-antisymmetry. We expect the study on the optical side could eventually shed light on the quantum-mechanical side, for interest of investigating $V(x,t) = -V^*(x,-t)$.

One may ask why in casting back the pseudo-$\mathcal{PT}$-antisymmetry to Schrödinger equation, both variables x and t are included in potential V, while in Eq. (2) only variable x is shown. This comes from the features of 1D atomic optical lattices, which cause the difference between paraxial wave equation and Schrödinger equation in spite of the isomorphism. Since the atomic lattices are constructed by forming dipole traps to trap the atoms, there is density distribution in transverse plane, which affects the complex refractive index n, so n is not only function of z, but also x. However along the z axis of atomic optical lattices, settlement on any value of x does not affect the pseudo-$\mathcal{PT}$-antisymmetry, so we can express n as $n(z)$.

3 Universal Pseudo-$\mathcal{PT}$-antisymmetry on One-dimensional Atomic Lattices

For any atomic configuration, the density matrix equations of off-diagonal terms can be expressed in the general form of master equation

$$\dot{\rho}_{nm} = -\frac{\mathrm{i}}{\hbar}[\hat{H}, \rho]_{nm} - \gamma_{nm}\rho_{nm}\,.$$

The Hamiltonian can be written as $\hat{H} = \hat{H}_0 + \hat{V}$, where $\hat{H}_0$ is the Hamiltonian of free atom, and $\hat{V}$ the interaction

between atom and applied fields. Then since $[\hat{H}_0, \rho]_{nm} = (E_n - E_m)\rho_{nm}$, the master equation becomes

$$\dot{\rho}_{nm} = -\mathrm{i}\omega_{nm}\rho_{nm} - \frac{\mathrm{i}}{\hbar}[\hat{V}, \rho]_{nm} - \gamma_{nm}\rho_{nm}\,, \qquad (7)$$

where $\omega_{nm} = (E_n - E_m)/\hbar = \omega_n - \omega_m$ is the resonant transition frequency between energy level n and m of the atom.

On 1D atomic lattices, we are applying a weak field to probe the optical response. Compared to all the other strong coupling fields, this is a perturbation, therefore we can turn to the traditional perturbative calculation method in nonlinear optics to carry out our calculation.

First suppose all external fields are treated as perturbation, then from Eq. (7), we have the first and second order perturbed ρ_{nm} expressed as

$$\rho^{(1)}_{nm} = \frac{-\mathrm{i}}{\hbar}\int_{-\infty}^{t} [\hat{V}(t'), \rho^{(0)}]_{nm}\, \mathrm{e}^{(\mathrm{i}\omega_{nm}+\gamma_{nm})(t'-t)}\,\mathrm{d}t'\,, \qquad (8)$$

$$\rho^{(2)}_{nm} = \frac{-\mathrm{i}}{\hbar}\int_{-\infty}^{t} [\hat{V}(t'), \rho^{(1)}]_{nm}\, \mathrm{e}^{(\mathrm{i}\omega_{nm}+\gamma_{nm})(t'-t)}\,\mathrm{d}t'\,, \qquad (9)$$

where the perturbation $\hat{V}(t)$ is defined as $\hat{V}(t') = -\boldsymbol{d}_{nm}\cdot\boldsymbol{E}(t')$, with $\boldsymbol{E}(t') = \boldsymbol{E}(\omega_{f(nm)})\,\mathrm{e}^{-\mathrm{i}\omega_{f(nm)}t'}$ being the field coupling energy states $|n\rangle$ and $|m\rangle$ on the relevant dipole moment $\boldsymbol{d}_{nm}$, and $\omega_{f(nm)}$ the frequency of the coupling field. Since we have

$$[\hat{V}(t'), \rho^{(0)}]_{nm} = -(\rho^{(0)}_{mm} - \rho^{(0)}_{nn})\boldsymbol{d}_{nm}\cdot\boldsymbol{E}(\omega_{f(nm)})\,\mathrm{e}^{-\mathrm{i}\omega_{f(nm)}t'}\,, \qquad (10)$$

therefore

$$\rho^{(1)}_{nm} = \frac{\mathrm{i}}{\hbar}(\rho^{(0)}_{mm} - \rho^{(0)}_{nn})\frac{\boldsymbol{d}_{nm}\cdot\boldsymbol{E}(\omega_{f(nm)})\,\mathrm{e}^{-\mathrm{i}\omega_{f(nm)}t}}{\mathrm{i}(\omega_{nm} - \omega_{f(nm)}) + \gamma_{nm}}\,, \qquad (11)$$

and we can derive from here

$$\boldsymbol{\chi}^{(1)}_{nm} = \frac{N}{\epsilon_0\hbar}(\rho^{(0)}_{mm} - \rho^{(0)}_{nn})\frac{\boldsymbol{d}_{mn}\boldsymbol{d}_{nm}}{(\omega_{nm} - \omega_{f(nm)}) - \mathrm{i}\gamma_{nm}}\,, \qquad (12)$$

where N is the atomic distribution function.

To get the second order perturbed density matrix term $\rho^{(2)}_{nm}$, normally we should directly bring the result of $\rho^{(1)}_{nm}$ into Eq. (9) for a second round calculation. But things get different here when using weak probe field approximation. Because the probe field is so small compared to the strong coupling fields, in the first round calculation of $\rho^{(1)}_{nm}$, we usually ignore the existance of the probe field. Then when calculating $\rho^{(2)}_{nm}$, we begin to include the effect of probe field. This is to say, the $\hat{V}(t')$ in Eq. (8) and Eq. (9) are different by an addition of probe field. And the optical response of the probe field is the difference between the original $\rho^{(2)}_{nm}$ without throwing in probe field

$$\rho^{(2)}_{nm} = \frac{-\mathrm{i}}{\hbar}\int_{-\infty}^{t} [\hat{V}(t'), \rho^{(1)}]_{nm}\, \mathrm{e}^{(\mathrm{i}\omega_{nm}+\gamma_{nm})(t'-t)}\,\mathrm{d}t'\,,$$

and that after throwing in the probe field

$$\rho^{(2)'}_{nm} = \frac{-\mathrm{i}}{\hbar}\int_{-\infty}^{t} [\hat{V}(t') + \delta\hat{V}(t'), \rho^{(1)}]_{nm}\, \mathrm{e}^{(\mathrm{i}\omega_{nm}+\gamma_{nm})(t'-t)}\,\mathrm{d}t'\,,$$

where under the assumption that the probe field is coupled to energy level $|k\rangle$ and $|l\rangle$,

$$\delta\hat{V}(t') = -\Sigma_{n,m}\boldsymbol{d}_{nm}\cdot\boldsymbol{E}_{\mathrm{probe}}(\omega_{f(kl)})\,\mathrm{e}^{-\mathrm{i}\omega_{f(kl)}t'} = -\boldsymbol{d}_{kl}\cdot\boldsymbol{E}_{\mathrm{probe}}(\omega_{f(kl)})\,\mathrm{e}^{-\mathrm{i}\omega_{f(kl)}t'}\,.$$

We then see the change of $\rho^{(2)}_{nm}$ by applying the weak probe field is

$$\delta\rho^{(2)}_{nm} = \frac{-\mathrm{i}}{\hbar}\int_{-\infty}^{t} [\delta\hat{V}(t'), \rho^{(1)}]_{nm}\, \mathrm{e}^{(\mathrm{i}\omega_{nm}+\gamma_{nm})(t'-t)}\,\mathrm{d}t'\,.$$

On the other hand, it is straightforward to get

$$[\delta\hat{V}(t'), \rho^{(1)}]_{kl} = -(\rho^{(1)}_{kk} - \rho^{(1)}_{ll})\boldsymbol{d}_{kl}\cdot\boldsymbol{E}(\omega_{f(kl)})\,\mathrm{e}^{-\mathrm{i}\omega_{f(kl)}t'},$$

since this is analogous to the expression in Eq. (10), comparing with

$$\boldsymbol{\chi}^{(1)}_{nm} = \frac{N}{\epsilon_0\hbar}(\rho^{(0)}_{mm} - \rho^{(0)}_{nn})\frac{\boldsymbol{d}_{mn}\boldsymbol{d}_{nm}}{(\omega_{nm} - \omega_{f(nm)}) - \mathrm{i}\gamma_{nm}}\,,$$

following the same path we have

$$\boldsymbol{\chi}^{(2)}_{kl} = \frac{N}{\epsilon_0\hbar}(\rho^{(1)}_{ll} - \rho^{(1)}_{kk})\frac{\boldsymbol{d}_{lk}\boldsymbol{d}_{kl}}{(\omega_{kl} - \omega_{f(kl)}) - \mathrm{i}\gamma_{kl}}\,. \qquad (13)$$

This is the expression of weak probe field susceptibility. Now we relate this to the spatial sinusoidal field detuning set. We get this idea from solving the zigzag-type configuration problems, which we will present as an example in the next section. We rewrite the above expression as

$$\boldsymbol{\chi}^{(2)}_{kl} = \mathrm{i}\frac{N}{\epsilon_0\hbar}(\rho^{(1)}_{ll} - \rho^{(1)}_{kk})\frac{\boldsymbol{d}_{lk}\boldsymbol{d}_{kl}}{\mathrm{i}(\omega_{kl} - \omega_{f(kl)}) + \gamma_{kl}}\,. \qquad (14)$$

The part $\mathrm{i}(\omega_{kl} - \omega_{f(kl)})$ in the denominator is by definition the term $\mathrm{i}\Delta_d$, where Δ_d is the frequency detuning of the probe field. So in a generalized way, we can say that the

denominator can be expressed as the polynomial in the indeterminate $\mathrm{i}\Delta_d$ in the form

$$\Sigma_l B_l(\mathrm{i}\Delta_d)^l\,,$$

knowing γ_{kl} can be looked on as $\gamma_{kl}(\mathrm{i}\Delta_d)^0$. On the other hand, for the numerator, both $\rho_{ll}^{(1)}$ and $\rho_{kk}^{(1)}$ are real numbers that can be expressed in form

$$\Sigma_{k=0} A_{2k}(\mathrm{i}\Delta_d)^{2k}\,,$$

which is a special case of $\Sigma_{j=0}A_j(\mathrm{i}\Delta_d)^j$. Therefore we can say the expression of Eq. (14) is a special case of expression

$$\boldsymbol{\chi}_{kl}^{(2)} = \mathrm{i}\frac{N\boldsymbol{d}_{lk}\boldsymbol{d}_{kl}}{\epsilon_0\hbar}\frac{\Sigma_{j=0}^{N_1}A_j(\mathrm{i}\Delta_d)^j}{\Sigma_{l=0}^{N_2}B_l(\mathrm{i}\Delta_d)^l}\,, \tag{15}$$

where N_1 is the highest order of indeterminate $\mathrm{i}\Delta_d$ in the numerator's polynomial, and N_2 the highest order of $\mathrm{i}\Delta_d$ in the denominator's polynomial. If we can prove that the expression in Eq. (15) can have the universal pseudo-$\mathcal{PT}$-antisymmetry, then it will also work on its special case, Eq. (14).

Equation (15) can be rewritten as

$$\boldsymbol{\chi}_{kl}^{(2)} = \mathrm{i}\frac{N\boldsymbol{d}_{lk}\boldsymbol{d}_{kl}}{\epsilon_0\hbar}\frac{m\Sigma_m[C_{2m}(\Delta_d)^{2m} + \mathrm{i}C_{2m+1}(\Delta_d)^{2m+1}]}{\Sigma_P D_{2p}(\Delta_d)^{2p}}\,, \tag{16}$$

where C_{2m}, C_{2m+1} $(m = 0,1,2,\ldots)$ and D_{2p} $(p = 0,1,2,\ldots)$ are real coefficients from rearranged polynomials of A_j $(j = 0,1,\ldots,N_1)$ and B_l $(l = 0,1,\ldots,N_2)$. Normally for 1D atomic lattices, $N = N(z)$ is the periodic Gaussian distribution function of the atom density, which can be expressed as

$$N(z) = N_0\,\mathrm{e}^{-(z-z_{0i})^2/\sigma^2}, \quad z \in \left[z_{0i} - \frac{a}{2}, z_{0i} + \frac{a}{2}\right], \tag{17}$$

where z_{0i} is the i-th lattice center, a the length of the lattice unit (also the spatial period of the 1D optical lattice), N_0 the density of atoms at lattice center, and σ the standard deviation of the Gaussian distribution. We can always choose an appropriate reference point z_0 (in this case, any z_{0i}) to make $N(z)$ an even function about z_0. After that, it is straightforward to see that if we set the coupling field frequency detuning Δ_d to be a sine function of z axis, i.e.,

$$\Delta_d = A\sin[2\pi(z - z_0)/a]\,, \tag{18}$$

where A represents the real amplitude of the oscillation, then about the reference point z_0 along z direction, $\mathrm{Re}[\chi_{kl}^{(2)}]$ is an odd function and $\mathrm{Im}[\chi_{kl}^{(2)}]$ is an even function, which indicates the realization of pseudo-$\mathcal{PT}$-antisymmetry $n(z) = -n^*(-z)$.

We have proved that under spatial sinusoidal detuning setting, a probe field susceptibility described by Eq. (15) will demonstrate pseudo-$\mathcal{PT}$-antisymmtry. Since under the weak probe field approximation, the probe susceptibility of 1D atomic lattices of any configuration can always be expressed by Eq. (14), a special case of Eq. (15), we have arrived at the conclusion that the sinusoidal detuning setting can induce universal pseudo-$\mathcal{PT}$-antisymmtry on 1D atomic optical lattices, regardless of energy level configuration.

In the next section we will present an example of universal pseudo-$\mathcal{PT}$-antisymmtry inducement on the zigzag-type configuration family of 1D atomic lattices, where we first found the idea of sinusoidal detuning setting in our early study, and where we got our first inspiration on the general case proof shown above.

4 Universal Pseudo-$\mathcal{PT}$-Antisymmetry on Zigzag-Type Configuration Family: An Example

4.1 *Case Study: N Configuration*

(i) ***The Model***

We first point out that the control of n is equivalent to modulating probe susceptibility χ_p. Since $n = \sqrt{1+\chi_p} \approx 1 + \chi_p/2$, and from Sec. 2 we know that $n = n_0 + \delta n$ with n_0 being the background refractive index, also for atomic optical lattices $n_0 = 1$, so we have $\delta n = \chi_p/2$.

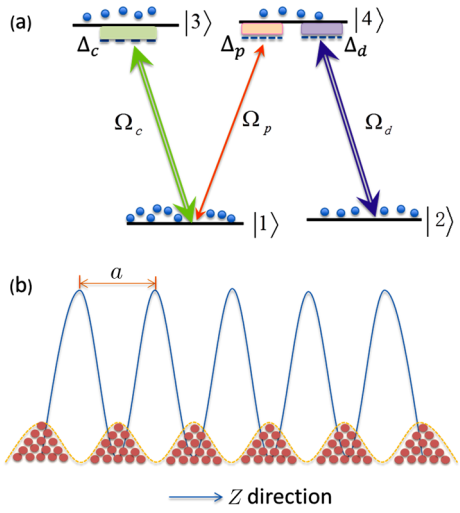

Fig. 1 (Color online) (a) Diagram of the four-level N configuration (4-zigzag), into which the atoms are driven by a weak probe field Ω_p and two moderate coupling field Ω_c and Ω_d. (b) An ensemble of cold ^{87}Rb atoms forming 1D optical lattice by being trapped at the bottom of periodically distributed dipole traps along z direction. The spatial period of the dipole trap distribution (and therefore the spatial period of atom distribution) is a. Within each dipole trap, we assume the atoms to be in Gaussian distribution, with σ being the standard deviation, as described by Eq. (17).

We design a system of one-dimensional optical lattice, composed of Gaussian-distributed bunches of cold ^{87}Rb atoms, with each bunch seated at the bottom of

a dipole trap along z direction, and atoms coherently driven into N-type configuration by three coherent laser fields applied to the system, at frequencies (amplitudes) ω_p ($\boldsymbol{E}_p$), ω_c ($\boldsymbol{E}_c$), and ω_d ($\boldsymbol{E}_d$), as shown in Figs. 1(a) and 1(b). The N-configuration consists of two ground levels $|1\rangle$ and $|2\rangle$ and two excited levels $|3\rangle$ and $|4\rangle$, and the weak probe field ω_p interacts with the dipole-allowed transition $|1\rangle \leftrightarrow |4\rangle$, while the two strong pump fields ω_c and ω_d act upon transitions $|1\rangle \leftrightarrow |3\rangle$ and $|2\rangle \leftrightarrow |4\rangle$, respectively. The corresponding frequency detunings are defined as $\Delta_p = \omega_p - \omega_{41}$, $\Delta_c = \omega_c - \omega_{31}$, $\Delta_d = \omega_d - \omega_{42}$, and the Rabi frequencies $\Omega_p = \boldsymbol{E}_p \cdot d_{14}/\hbar$, $\Omega_c = \boldsymbol{E}_c \cdot d_{13}/\hbar$, and $\Omega_d = \boldsymbol{E}_d \cdot d_{24}/\hbar$, with $\omega_{ij} = \omega_i - \omega_j$ being resonant transition frequencies and d_{ij} the relevant dipole moments (i, j are labels of the energy levels).

With rotating-wave and electric-dipole approximations, the interaction Hamiltonian can be written as

$$\hat{H}_I = -\hbar[(\Delta_p - \Delta_d)|2\rangle\langle 2| + \Delta_c|3\rangle\langle 3| + \Delta_p|4\rangle\langle 4|] - \hbar[\Omega_c|3\rangle\langle 1| + \Omega_p|4\rangle\langle 1| + \Omega_d|4\rangle\langle 2| + \text{h.c.}]\,.$$

We then get the density matrix equations:

$$\begin{aligned}
\partial_t\rho_{11} &= +\Gamma_{31}\rho_{33} + \Gamma_{41}\rho_{44} + \mathrm{i}\Omega_c^*\rho_{31} - \mathrm{i}\Omega_c\rho_{13} + \mathrm{i}\Omega_p^*\rho_{41} - \mathrm{i}\Omega_p\rho_{14}\,,\\
\partial_t\rho_{22} &= +\Gamma_{32}\rho_{33} + \Gamma_{42}\rho_{44} + \mathrm{i}\Omega_d^*\rho_{42} - \mathrm{i}\Omega_d\rho_{24}\,,\\
\partial_t\rho_{33} &= -\Gamma_{31}\rho_{33} - \Gamma_{32}\rho_{33} + \mathrm{i}\Omega_c\rho_{13} - \mathrm{i}\Omega_c^*\rho_{31}\,,\\
\partial_t\rho_{12} &= -\gamma_{12}'\rho_{12} + \mathrm{i}\Omega_c^*\rho_{32} + \mathrm{i}\Omega_p^*\rho_{42} - \mathrm{i}\Omega_d\rho_{14}\,,\\
\partial_t\rho_{13} &= -\gamma_{13}'\rho_{13} + \mathrm{i}\Omega_p^*\rho_{43} + \mathrm{i}\Omega_c^*(\rho_{33} - \rho_{11})\,,\\
\partial_t\rho_{14} &= -\gamma_{14}'\rho_{14} + \mathrm{i}\Omega_c^*\rho_{34} + \mathrm{i}\Omega_p^*(\rho_{44} - \rho_{11}) - \mathrm{i}\Omega_d^*\rho_{12}\,,\\
\partial_t\rho_{23} &= -\gamma_{23}'\rho_{23} + \mathrm{i}\Omega_d^*\rho_{43} - \mathrm{i}\Omega_c^*\rho_{21}\,,\\
\partial_t\rho_{24} &= -\gamma_{24}'\rho_{24} - \mathrm{i}\Omega_p^*\rho_{21} + \mathrm{i}\Omega_d^*(\rho_{44} - \rho_{22})\,,\\
\partial_t\rho_{34} &= -\gamma_{34}'\rho_{34} + \mathrm{i}\Omega_c\rho_{14} - \mathrm{i}\Omega_p^*\rho_{31} - \mathrm{i}\Omega_d^*\rho_{32}\,,
\end{aligned} \tag{19}$$

where $\gamma_{12}' = \gamma_{12} + \mathrm{i}\Delta_{12}$, $\gamma_{13}' = \gamma_{13} + i\Delta_c$, $\gamma_{14}' = \gamma_{14} + \mathrm{i}\Delta_p$, $\gamma_{23}' = \gamma_{23} + \mathrm{i}\Delta_{23}$, $\gamma_{24}' = \gamma_{24} + \mathrm{i}\Delta_d$, $\gamma_{34}' = \gamma_{34} + \mathrm{i}\Delta_{34}$; and $\Delta_{12} = \Delta_p - \Delta_d$, $\Delta_{23} = \Delta_c + \Delta_d - \Delta_p$, $\Delta_{34} = \Delta_p - \Delta_c$. We also assume $\Gamma_{31} = \Gamma_{32} = \Gamma_{41} = \Gamma_{42} = \gamma$, and $\gamma_{12} \ll \gamma$, therefore $\gamma_{13} = \gamma_{14} = \gamma_{23} = \gamma_{24} = \gamma$, $\gamma_{34} = 2\gamma$. Closure of this atomic system requires that $\rho_{ij} = \rho_{ji}^*$ and $\rho_{11} + \rho_{22} + \rho_{33} + \rho_{44} = 1$.

(ii) ***A Special Case of Pseudo-$\mathcal{PT}$-Antisymmetry on N Configuration***

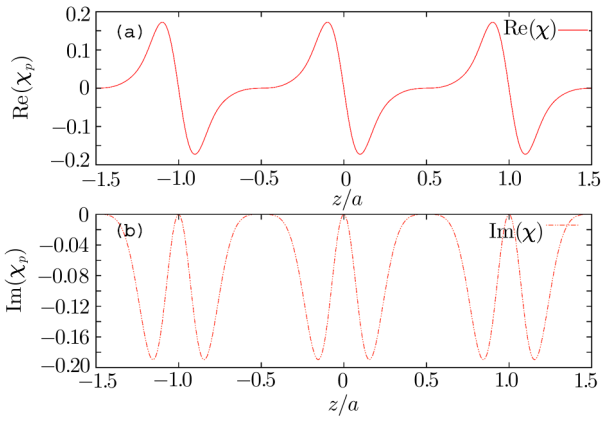

Fig. 2 (Color online) The pseudo-$\mathcal{PT}$-antisymmetry of $\chi_p(z)$ under condition of Eq. (18). (a) The real part of probe susceptibility $\mathrm{Re}[\chi_p]$ for N configuration as function of z, with x axis in unit of z/a. (b) The imaginary part of probe susceptibility $\mathrm{Im}[\chi_p]$ for N configuration as function of z, with x axis in unit of z/a. Here we set $z_0 = 0$ and $A = 1$ MHz in $\Delta_d = A\sin[2\pi(z - z_0)/a]$, $\Omega_c = \Omega_d = 5$ MHz, $\Omega_p = 0.06$ MHz, and $\Gamma_{31} = \Gamma_{32} = \Gamma_{41} = \Gamma_{42} = 3$ MHz. We take $\sigma = 0.2a$ in Gaussian distribution function of Eq. (17).

Using weak probe field approximation, we obtain the first-order steady-state solutions of Eqs. (19), and since we are interested in the probe field, we directly go for the expression of $\rho_{14}^{(1)}$. For simplicity, we set $\gamma_{12} = 0$ and look at the special case

$$\Omega_c = \Omega_d, \quad \Delta_c = \Delta_d, \quad \Delta_p = 0\,, \tag{20}$$

then obtain

$$\rho_{14} = \mathrm{i}\Omega_p^*\left\{\frac{\Omega_d(\gamma + \mathrm{i}\Delta_d)(\gamma - 2\mathrm{i}\Delta_d)\{-\Omega_c^*\mathrm{i}\Delta_d[\Omega_c^2 - \mathrm{i}\Delta_d(\gamma - 2\mathrm{i}\Delta_d)] + \Omega_d^*\Omega_c^2(2\gamma - \mathrm{i}\Delta_d)\}}{2(2\Omega_d^2 + \Delta_d^2 + \gamma^2)\{[\Omega_c^2(2\gamma - \mathrm{i}\Delta_d) - \mathrm{i}\Delta_d\Omega_d^2][\gamma(\Omega_c^2 - \mathrm{i}\Delta_d(\gamma - 2\mathrm{i}\Delta_d)) + (\gamma - 2\mathrm{i}\Delta_d)\Omega_d^2] - \Delta_d^2\Omega_c^2(\gamma - 2\mathrm{i}\Delta_d)^2\}}\right.$$
$$\left. - \frac{(\gamma^2 + \Delta_d^2)[\Omega_c^2 - \mathrm{i}\Delta_d(\gamma - 2\mathrm{i}\Delta_d)][\Omega_c^2(2\gamma - \mathrm{i}\Delta_d) - \mathrm{i}\Delta_d\Omega_d^2]}{2(2\Omega_d^2 + \Delta_d^2 + \gamma^2)\{[\Omega_c^2(2\gamma - \mathrm{i}\Delta_d) - \mathrm{i}\Delta_d\Omega_d^2][\gamma(\Omega_c^2 - \mathrm{i}\Delta_d(\gamma - 2\mathrm{i}\Delta_d)) + (\gamma - 2\mathrm{i}\Delta_d)\Omega_d^2] - \Delta_d^2\Omega_c^2(\gamma - 2\mathrm{i}\Delta_d)^2\}}\right\}. \tag{21}$$

Here we have uniformly replaced all the Δ_c by Δ_d, while still writing down Ω_c and Ω_d separately. The reason of doing this will be explained later.

We can see that under the assumption that $\Omega_c = \Omega_d$ are real numbers, both the numerator and the denominator of the formula can be expressed as polynomials in indeterminate $\mathrm{i}\Delta_d$, i.e.,

$$\rho_{14} = \mathrm{i}\Omega_p^*\frac{\Sigma_{j=0}^{N_1}A_j(\mathrm{i}\Delta_d)^j}{\Sigma_{l=0}^{N_2}B_l(\mathrm{i}\Delta_d)^l}\,, \tag{22}$$

where N_1 is the highest order of term $\mathrm{i}\Delta_d$ in numerator, and N_2 the highest order of $\mathrm{i}\Delta_d$ in denominator. A_j ($j = 0, 1, \ldots, N_1$) and B_l ($l = 0, 1, \ldots, N_2$) are real coefficients determined by Eq. (21). The expression of Eq. (22) goes back to the form of Eq. (17), using $\chi_p = N|d_{14}|^2\rho_{41}/2\epsilon_0\hbar\Omega_p$ and setting $N(z)$ to be the periodic Gaussian distribution function described by Eq. (17), we realize pseudo-$\mathcal{PT}$-antisymmetry $n(z) = -n^*(-z)$ for 1D optical lattice on N-configuration.

In Figs. 2(a) and 2(b) we plot the real and imaginary parts of probe susceptibility χ_p as function of z. The parameters used here are $\Omega_c = \Omega_d = 5$ MHz, $\Omega_p = 0.06$ MHz, $\Gamma_{31} = \Gamma_{32} = \Gamma_{41} = \Gamma_{42} = 3$ MHz. For the frequency detuning function $\Delta_d = A\sin[2\pi(z - z_0)/a]$,

we choose $z_0 = 0$ and set $A = 1$ MHz.

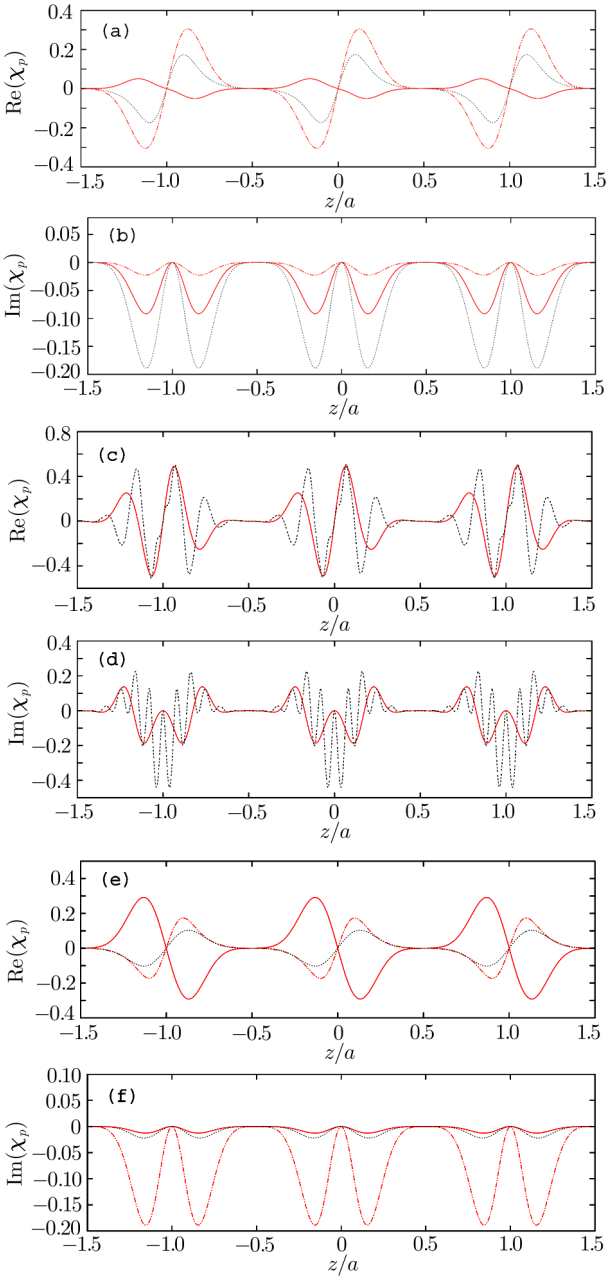

Fig. 3 (Color online) (a) and (b) are the real and imaginary parts of $\chi_p(z)$ under different oscillation amplitudes of Δ_c and Δ_d. The red solid line corresponds to $A_1/A_2 = 0.3$, black dashed line corresponds to $A_1/A_2 = 1$, and orange dashed line corresponds to $A_1/A_2 = 3$ in Eqs. (23). (c) and (d) are the real and imaginary parts of $\chi_p(z)$ under different spatial periods of Δ_c and Δ_d. Red solid line corresponds to $m = 3$, $n = 1$, gray dashed line corresponds to $m = 5$, $n = 7$ in Eqs. (24). (e) and (f) are the real and imaginary parts of $\chi_p(z)$ under different values of Ω_c and Ω_d. Red solid line corresponds to $\Omega_c = 3$ MHz, $\Omega_d = 6$ MHz, orange dashed line corresponds to $\Omega_c = 5$ MHz, $\Omega_d = 5$ MHz, black dashed line corresponds to $\Omega_c = 7$ MHz, $\Omega_d = 2$ MHz. All the other parameters are the same as in Fig. 2.

(iii) ***Pseudo-$\mathcal{PT}$-Antisymmetry on N Configuration under Modified Parameters***

Setting Δ_c=Δ_d in Eq. (20) ensures the expression of ρ_{14} in Eq. (21) to be a function of indeterminate iΔ_d, however, loosening this condition to

$$\Delta_c = A_1 \sin[2\pi(z - z_0)/a]\,,$$
$$\Delta_d = A_2 \sin[2\pi(z - z_0)/a]\,, \tag{23}$$

where $A_1 \neq A_2$ are both real amplitudes, we still get the pseudo-$\mathcal{PT}$-antisymmetry, as shown in Figs. 3(a) and 3(b).

We can also modify the periods instead of amplitudes of the sine functions by setting

$$\Delta_c = A \sin[2\pi m(z - z_0)/a]\,,$$
$$\Delta_d = A \sin[2\pi n(z - z_0)/a]\,, \tag{24}$$

where m and n are different integers, and we get the modulated periodical spatial distribution of χ_p, which still satisfies the pseudo-$\mathcal{PT}$-antisymmetry as shown in Figs. 3(c) and 3(d).

For the condition $\Omega_c = \Omega_d$ in Eq. (20), we change them to different values and still get the pseudo-$\mathcal{PT}$-antisymmetry. The results are shown in Figs. 3(e) and 3(f).

4.2 *Numerical Study on Different Zigzag Configurations*

We now look at the different zigzag-type atom configurations as shown in Fig. 4, on the same setting of optical lattice described by Fig. 1(a). In Fig. 4(a) we show the M-type zigzag configuration, which is the original N-type configuration spreading out one "leg" on the left-hand side to an additional ground level state (labeled $|1\rangle$ here). Figure 4(b) is the N-type configuration spreading out one "leg" on the right-hand side to an additional excited level (labeled $|5\rangle$ here), which we call W-type configuration. Combining these two, the N-type spreading out one "leg" to each side gives the six-level zigzag type in Fig. 4(c). And lastly, adding one more "leg" on the right-hand side of six-level zigzag gives seven-level zigzag in Fig. 4(d).

For convenient comparison between different configuration types, we assume that in and between each type:

(i) All the Rabi frequencies Ω_{c_i} and Ω_{d_i} (i is integer) are of equal values.

(ii) All the lower level states are treated as ground states, and for integer i, j representing different ground states, $\gamma_{ij} = 0$.

(iii) Γ_{ij} (i, j are different integers) only exists between adjacent excited and ground states that are coupled by external fields.

Notice that if we also include the N-type into the current group for comparison, we should set $\Gamma_{32} = 0$, which is different from the N-type setting previously used in this section.

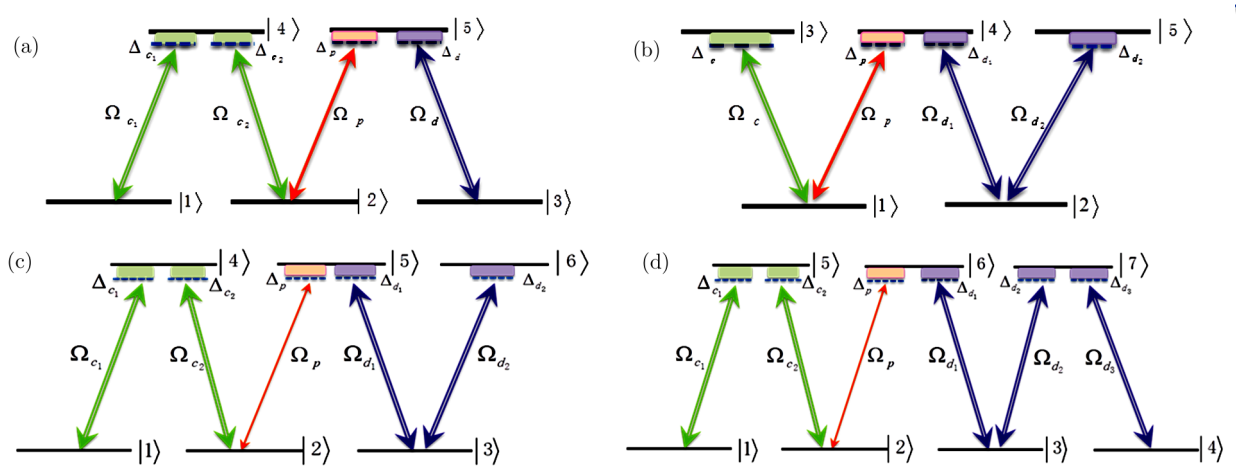

Fig. 4 (Color online) (a) M-type zigzag configuration, which is N-type configuration spreading out one "leg" on the left-hand side to the newly added ground state labeled $|1\rangle$. (b) W-type zigzag configuration, which is N-type configuration spreading out one "leg" on the right-hand side to the newly added excited state labeled $|5\rangle$. (c) Six-level zigzag configuration, which is N-type configuration spreading out one "leg" on the left-hand side to the newly added ground state labeled $|1\rangle$, and one "leg" on the right-hand side to the newly added excited state labeled $|6\rangle$. (d) Seven-level zigzag configuration, which is six-level zigzag configuration spreading out one "leg" on the right-hand side to the newly added ground state labeled $|4\rangle$.

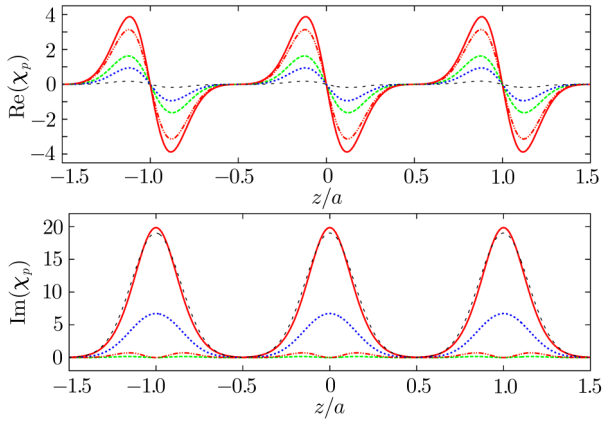

Fig. 5 (Color online) The pseudo-$\mathcal{PT}$-antisymmetry of $\chi_p(z)$ on N-type (red solid line), M-type (green dashed line), W-type (blue dotted line), six-level zigzag (black dotted line) and seven-level zigzag (orange dashed line) atom configurations. (a) The real part of probe susceptibility $\mathrm{Re}[\chi_p]$ for different atom configurations as function of z, with x axis in unit of z/a. (b) The imaginary part of probe susceptibility $\mathrm{Im}[\chi_p]$ for different atom configurations as function of z, with x axis in unit of z/a. The parameters used here are $\Omega_{c_i} = \Omega_{d_i} = 5$ MHz, $\Omega_p = 0.06$ MHz, $\Gamma_{ij} = 3$ MHz (when being nonzero term), $\Delta_{c_i} = \Delta_{d_i} = A\sin[2\pi(z - z_0)/a]$ with $z_0 = 0$ and $A = 1$ MHz. The atom density distribution function is the periodic Gaussian function given by Eq. (17) and $\sigma = 0.2a$.

Following these setting, in drawing the plot of Fig. 5, we set $\Omega_{c_i} = \Omega_{d_i} = 5$ MHz, $\Omega_p = 0.06$ MHz, $\Gamma_{ij} = 3$ MHz whenever it is nonzero, and for the key role of coupling field detunings, we set

$$\Delta_{c_i} = \Delta_{d_i} = \Delta = A\sin[2\pi(z - z_0)/a]\,, \qquad (25)$$

and choose $z_0 = 0$ and $A = 1$ MHz. The periodic Gaussian distribution function of atom density on the optical lattice is still given by Eq. (17). The uniform inducement of pseudo-$\mathcal{PT}$-antisymmetry on different zigzag-type atomic optical lattices are shown in Fig. 5.

From Fig. 5 we see that the N-type configuration has the largest amplitude in both real and imaginary parts of probe susceptibility χ_p. The M-type and W-type are both N-type spreading out one "leg", one to an extra ground state, one to an excited state. Compared to N-type, the W-type has both the real and imaginary parts of χ_p suppressed to a moderate level, while for the M-type, the real part of χ_p is also suppressed largely but less than the W-type, however the imaginary part is suppressed almost to zero. The six-level zigzag configuration is the W-type spreading out one "leg" to an extra ground state, and the seven-level zigzag configuration is the six-level configuration spreading out one more "leg" to a ground state on the other side. Compared to the W-type, the real part of χ_p of six-level configuration is strongly suppressed, but that of seven-level is strongly enlarged. On the contrary, the imaginary part of χ_p of six-level configuration is strongly enlarged, and that of seven-level is strongly suppressed. We leave the detailed and systematic study of the correlation between the atom configuration and probe susceptibility to the future work.

5 Conclusions

In this paper, we show the result that under the setting of sinusoidal spatial distribution of coupling field detunings, the pseudo-$\mathcal{PT}$-antisymmetry, i.e. $\delta n(z) = -\delta n^*(-z)$, the complex refractive index antisymmetry along propagation direction of 1D atomic lattices, can be

universally induced on the 1D atomic lattices of any configuration.

We find that the reason for the uniform inducement of pseudo-$\mathcal{PT}$-antisymmetry is rooted in the quantum-mechanical nature of atom-field interaction, which can be derived directly from the general form of master equation under weak probe field approximation.

For future interest of the universal pseudo-$\mathcal{PT}$-antisymmetry, we also point out that when being cast back to quantum-mechanical side, $\delta n(z) = -\delta n^*(-z)$ corresponds to $V(x,t) = -V^*(x,-t)$, the conjugate time-reversal antisymmetry of complex potential $V(x,t)$ in 1D Schrödinger equation.

In conclusion, the universal inducement of pseudo-$\mathcal{PT}$-antisymmetry is a novel observation. It expands our understanding of the origin of optical response of atomic lattices, provides more reliable and variable method in designing atomic optical lattices, and offers more flexibility and stability to the optical features of atomic lattices.

Acknowledgements

X. Wang would like to thank Jilin University and Center for Quantum Sciences of Northeast Normal University, where this work was first started.

References

[1] C. M. Bender and S. Boettcher, Phys. Rev. Lett. **80** (1998) 5243.

[2] C. M. Bender, D. C. Brody, and H. F. Jones, Phys. Rev. Lett. **89** (2002) 270401.

[3] S. Weigert, J. Opt. B: Quantum Semiclass. Opt. **5** (2003) S416.

[4] K. Jones-Smith and H. Mathur, Phys. Rev. A **82** (2010) 042101.

[5] S. Ibáñez and J. G. Muga, Phys. Rev. A **89** (2014) 033403.

[6] A. A. Zyablovsky, A. P. Vinogradov, A. V. Dorofeenko, *et al.*, Phys. Rev. A **89** (2014) 033808.

[7] S. Garmon, M. Gianfreda, and N. Hatano, Phys. Rev. A **92** (2015) 022125.

[8] O. Vázquez-Candanedo, J. C. Hernández-Herrejón, F. M. Izrailev, and D. N. Christodoulides, Phys. Rev. A **89** (2014) 013832.

[9] A. Dasarathy, J. P. Isaacson, K. Jones-Smith, J. Tabachnik, and H. Mathur, Phys. Rev. A **87** (2013) 062111.

[10] F. Correa, V. Jakubský, and M. S. Plyushchay, Phys. Rev. A **92** (2015) 023839.

[11] J. E. Elenewski and H. Chen, Phys. Rev. B **90** (2014) 085104.

[12] B. Zhu, R. Lü, and S. Chen, Phys. Rev. A **89** (2014) 062102.

[13] K. G. Makris, R. El-Ganainy, D. N. Christodoulides, and Z. H. Musslimani, Phys. Rev. Lett. **100** (2008) 103904.

[14] A. Regensburger, C. Bersch, M. A. Miri, *et al.*, Nature (London) **488** (2012) 167.

[15] S. Klaiman, U. Günther, and N. Moiseyev, Phys. Rev. Lett. **101** (2008) 080402.

[16] C. E. Rüter, K. G. Makris, R. El-Ganainy, *et al.*, Nat. Phys. **6** (2010) 192.

[17] N. I. Landy, S. Sajuyigbe, J. J. Mock, *et al.*, Phys. Rev. Lett. **100** (2008) 207402.

[18] Y. D. Chong, L. Ge, H. Cao, and A. D. Stone, Phys. Rev. Lett. **105** (2010) 053901.

[19] S. Longhi, Phys. Rev. A **82** (2010) 031801(R).

[20] Z. Lin, H. Ramezani, T. Eichelkraut, *et al.*, Phys. Rev. Lett. **106** (2011) 213901.

[21] L. Feng, Y. L. Xu, W. S. Fegadolli, *et al.*, Nat. Mater. **12** (2013) 108.

[22] C. Hang, G. X. Huang, and V. V. Konotop, Phys. Rev. Lett. **110** (2013) 083604.

[23] J. T. Sheng, M. A. Miri, D. N. Christodoulides, and M. Xiao, Phys. Rev. A **88** (2013) 041803(R).

[24] H. J. Li, J. P. Dou, and G. X. Huang, Opt. Express **21** (2013) 32053.

[25] J. H. Wu, M. Artoni, and G. C. La Rocca, Phys. Rev. Lett. **113** (2014) 123004.

[26] J. H. Wu, M. Artoni, and G. C. La Rocca, Phys. Rev. A **91** (2015) 033811.

[27] K. G. Makris, R. El-Ganainy, D. N. Christodoulides, and Z. H. Musslimani, Phys. Rev. Lett. **100** (2008) 103904.

[28] Z. H. Musslimani, K. G. Makris, R. El-Ganainy, and D. N. Christodoulides, Phys. Rev. Lett. **100** (2008) 030402.

[29] A. Guo, G. J. Salamo, D. Duchesne, *et al.*, Phys. Rev. Lett. **103** (2009) 093902.

[30] K. G. Makris, R. El-Ganainy, D. N. Christodoulides, and Z. H. Musslimani, Phys. Rev. A **81** (2010) 063807.

[31] A. Regensburger, M. A. Miri, C. Bersch, *et al.*, Phys. Rev. Lett. **110** (2013) 223902.

[32] B. Peng, S. K. Ozdemir, F. Lei, *et al.*, Nat. Phys. **10** (2014) 394.

[33] H. Alaeian and J. A. Dionne, Phys. Rev. B **89** (2014) 075136.

[34] S. Nixon and J. Yang, Phys. Rev. A **91** (2015) 033807.